Probing the nonlocal approximation to resonant collisions of electrons with diatomic molecules

Karel Houfek*
Institute of Theoretical Physics, Faculty of Mathematics and Physics, Charles University Prague, V Holešovičkách 2, 180 00 Praha 8, Czech Republic

T. N. Rescigno†
Chemical Sciences, Lawrence Berkeley National Laboratory, Berkeley, California 94720, USA

C. W. McCurdy‡
Department of Applied Science and Department of Chemistry, University of California, Davis, California 95616, USA and Chemical Sciences, Lawrence Berkeley National Laboratory, Berkeley, California 94720, USA
(Received 19 September 2007; published 16 January 2008)

A numerically solvable two-dimensional model introduced by the authors [Phys. Rev. A **73**, 032721 (2006)] is used to investigate the validity of the nonlocal approximation to the dynamics of resonant collisions of electrons with diatomic molecules. The nonlocal approximation to this model is derived in detail, all underlying assumptions are specified, and explicit expressions for the resonant and nonresonant (background) T matrix for the studied processes are given. Different choices of the so-called discrete state, which fully determines the nonlocal approximation, are discussed, and it is shown that a physical choice of this state can in general give poorer results than other choices that minimize the nonadiabatic effects and/or the background terms of the T matrix. Background contributions to the T matrix, which are usually not considered in the resonant theory of electron-molecule collisions, can contribute significantly not only to elastic but also to vibrational excitation cross sections. Dissociative attachment cross sections, however, are found to be properly described in the nonlocal model with any choice of discrete state that minimizes the importance of nonadiabatic effects and goes to the proper limit at large internuclear separation.

DOI: 10.1103/PhysRevA.77.012710 PACS number(s): 34.80.Ht, 34.80.Gs

I. INTRODUCTION

In a previous paper [1] (referred to hereafter as paper I), we introduced a simple two-dimensional model of electron collisions with diatomic molecules which enabled us to study the dynamics of inelastic resonant processes such as vibrational excitation

$$e^- + AB(v_\mathrm{i}) \to e^- + AB(v_\mathrm{f}) \tag{1}$$

and dissociative electron attachment

$$e^- + AB(v_\mathrm{i}) \to A + B^-. \tag{2}$$

The advantage of this model with one electronic and one nuclear degree of freedom is that we can solve it exactly, without the Born-Oppenheimer approximation, using appropriate numerical techniques developed recently by Rescigno and McCurdy [2,3]. Therefore, within our model we are able to obtain the essentially exact cross sections of the studied processes (1) and (2). Accordingly we can use this model to compare various approximate methods that have been employed to calculate the cross sections for resonant electron-molecule collisions, in particular the often used local complex potential (LCP) approximation [4,5] and the more sophisticated nonlocal, complex, and energy-dependent potential approximation (we refer to this approximation as the *nonlocal approximation* for brevity) on which the nonlocal resonance model of Domcke *et al.* is based (see [6] and references therein).

In I we defined a model Hamiltonian and constructed N_2-like and NO-like models embracing all essential features of the corresponding real electron-molecule systems. As expected, the LCP approximation, defined from the exact energy of the pole of the S matrix for fixed-nuclei electron scattering, yielded satisfactory results for energies sufficiently above threshold but failed to reproduce the energy dependence of the cross sections near threshold.

In this paper, we focus on a detailed study of the nonlocal approximation based on the Feshbach projection-operator formalism [6] and its comparison with the exact results of the two-dimensional model calculations. For that purpose, we give a thorough derivation of the nonlocal approximation to the two-dimensional model in Sec. III and write an explicit decomposition of the T matrix for vibrational excitation into *background* and *resonant* terms. It will be shown that the background terms, which were usually considered only for elastic scattering, can play an important role even for the inelastic vibrational excitation process.

The nonlocal approximation is completely determined by the so-called discrete state (we assume only one isolated resonance in our work). Once this state is given for all internuclear distances, other quantities appearing in the nonlocal approximation can be at least in principle calculated. The same numerical techniques that we used for solving the two-dimensional problem can be efficiently applied to solve the nonlocal approximation equations (see Sec. IV for details) and thus we are able to obtain reliable results for any given

*houfek@mbox.troja.mff.cuni.cz
†tnrescigno@lbl.gov
‡cwmccurdy@lbl.gov

discrete state. Several alternative definitions of the discrete state can be found in the literature (see, for example, [7–11]) including the unique definition of Lippmann and O'Malley [12] based on the physical significance of this state. But implementation of these definitions is elaborate and it is not the purpose of this paper to decide which of these definitions gives the best nonlocal approximation. Instead, we decided to investigate the nonlocal approximation by choosing several different discrete states which vary with the internuclear distance in a well-defined way, and it will be shown in Sec. VI that the *physical* choice of the discrete state as a square-integrable function which approximates the electronic wave function calculated at the resonant energy does not in general give better results than the other, quite arbitrary, choices of the discrete state. On the contrary, we will provide evidence that the smoothness of the discrete state and of the orthogonal electronic continuum states is essential to obtain quantitatively correct results within the nonlocal approximation but only if the contributions of background terms are properly included.

II. SUMMARY OF THE TWO-DIMENSIONAL MODEL

The detailed description of our two-dimensional model was given in I. Here we briefly summarize basic equations to define quantities needed for a discussion of the nonlocal resonance theory. We should note that the normalization of continuum states used here is different from that used in I, to be consistent with the energy normalization chosen in other papers dealing with the nonlocal theory.

We denote the unperturbed energy-normalized electronic continuum states by

$$\mathcal{J}_k^l(r) = \sqrt{\frac{2k}{\pi}}\, r j_l(kr) \tag{3}$$

where k denotes the electron momentum, l is the electron angular momentum, and j_l is the spherical Bessel function of the first kind [13] [in I the continuum states were chosen to be $rj_l(kr)$]. We consider molecular angular momenta to be zero; thus the unperturbed energy-normalized molecular-anion continuum state is simply

$$\mathcal{E}_K(R) = \sqrt{\frac{2\mu}{\pi K}}\sin(KR) \tag{4}$$

where K is the relative momentum of A and B^- in the dissociative attachment channel and μ denotes the reduced mass of the molecule AB. In accord with the energy normalization, the definition of the cross sections must also be changed (see below).

The full Hamiltonian of our model of the system $e^- + AB$ is

$$H = H_0 + V_{\text{int}}(R,r), \tag{5}$$

$$H_0 = T_R + V_0(R) + T_r + \frac{l(l+1)}{2r^2}, \tag{6}$$

where

$$T_R = -\frac{1}{2\mu}\frac{d^2}{dR^2}, \quad T_r = -\frac{1}{2}\frac{d^2}{dr^2} \tag{7}$$

are kinetic energy operators and R and r denote the molecular and electronic coordinates, respectively.

The exact wave function describing the model system at a given energy $E = E_{v_i} + E_i$ can be written as

$$|\Psi^+\rangle = |\chi_{v_i}\mathcal{J}_{k_i}^l\rangle + \frac{1}{E - H + i\eta}V_{\text{int}}|\chi_{v_i}\mathcal{J}_{k_i}^l\rangle, \tag{8}$$

where $\chi_{v_i}(R)$ is an initial vibrational state of the neutral molecule [an eigenfunction of $T_R + V_0(R)$] and $\mathcal{J}_{k_i}^l$ describes an incoming electron with momentum k_i. The wave function $\Psi_E^+(R,r)$ given by Eq. (8) is obviously an eigenfunction of the full Hamiltonian H with energy E.

The T matrices for vibrational excitation and dissociative attachment are given by

$$T_{v_i \to v_f}^{\text{VE}}(E) = \langle \chi_{v_f}\mathcal{J}_{k_f}^l | V_{\text{int}} | \Psi^+\rangle, \tag{9}$$

$$T_{v_i}^{\text{DA}}(E) = \langle \mathcal{E}_{K_{\text{DA}}}\phi_b | V_0 + V_{\text{int}} - V_b | \Psi^+\rangle, \tag{10}$$

where χ_{v_f} and $\mathcal{J}_{k_f}^l(r)$ are the final vibrational and electronic states, respectively. $\mathcal{E}_{K_{\text{DA}}}(R)$ describes the relative motion of the nuclei with the momentum K_{DA} and $\phi_b(r)$ is a bound state of the electron, both in the dissociative attachment channel. We assume there is only one electronic bound state $\phi_b(r)$ satisfying the equation

$$\left(T_r + \frac{l(l+1)}{2r^2} + V_b(r)\right)\phi_b(r) = -E_a\phi_b(r), \tag{11}$$

where $V_b(r)$ is given as the limit of the interaction potential for very large internuclear distances,

$$V_b(r) = \lim_{R\to\infty} V_{\text{int}}(R,r), \tag{12}$$

and E_a is the electron affinity of the "atom" B.

Finally we give the formulas for the cross sections,

$$\sigma_{v_i \to v_f}^{\text{VE}}(E) = \frac{4\pi^3}{k_i^2}|T_{v_i \to v_f}^{\text{VE}}(E)|^2, \tag{13}$$

$$\sigma_{v_i}^{\text{DA}}(E) = \frac{4\pi^3}{k_i^2}|T_{v_i}^{\text{DA}}(E)|^2 \tag{14}$$

with coefficients corresponding to the choice of energy-normalized continuum states.

III. THEORY OF THE NONLOCAL APPROXIMATION

The basic assumption leading to the nonlocal resonance theory of electron-molecule collisions [6] is the formation of a metastable molecular anion $(AB)^-$ during the collision, i.e., the electron is captured by the molecule into a quasibound (resonant) state which can be approximately described by a normalized square-integrable wave function. The derivation of the nonlocal resonance theory is then based on the Fesh-

bach projection-operator formalism [14,15] with operators chosen to project on the *resonant* and *nonresonant* parts of the electronic Hilbert space.

Here, we will proceed in three steps. First we define projection operators Q and P playing a central role in the Feshbach theory of resonance processes. Then we decompose the scattering T matrix into the resonant and background (nonresonant) terms and give explicit formulas for them. Finally, we derive the effective one-dimensional Schrödinger equation describing the nuclear dynamics of the resonance state $(AB)^-$ in a nonlocal, complex, and energy-dependent potential. The solution of this basic equation of the nonlocal resonance theory contains all information needed for calculation of resonance contributions to the vibrational excitation and dissociative attachment cross sections within the Born-Oppenheimer approximation.

A. Projection operators Q and P

The operator Q projecting on the resonant part $\mathcal{Q}$ of the electronic Hilbert space $\mathcal{H}_{\rm el}$ is given by

$$Q = |\phi_d\rangle\langle\phi_d|, \tag{15}$$

where $\phi_d(r;R)$ is a normalized, square-integrable, and in general complex wave function approximately describing the electron in a resonant state after being captured by the molecule. To simplify our derivation, we assume that there is a single isolated electronic resonance state becoming a bound state for large internuclear distances, which is true for all our models.

The projector P on the complementary (nonresonant or background) part $\mathcal{P}$ of $\mathcal{H}_{\rm el}$ is simply

$$P = 1 - Q. \tag{16}$$

Let us now define energy-normalized electronic states $\phi_k^+(r;R)$ as the eigenstates of the electronic Hamiltonian

$$H_{\rm el} = T_r + \frac{l(l+1)}{2r^2} + V_{\rm int}(R,r) \tag{17}$$

restricted on the $\mathcal{P}$ space, i.e.,

$$PH_{\rm el}P|\phi_k^+\rangle = \frac{k^2}{2}|\phi_k^+\rangle, \tag{18}$$

where a boundary condition for ϕ_k^+ is determined by the incoming wave $\mathcal{J}_k^I(r)$. In terms of the states ϕ_k^+, which are usually called *background* scattering states, the projector P can be expressed in the form

$$P = \int |\phi_k^+\rangle\langle\phi_k^+| k\, dk. \tag{19}$$

In a similar way we define electronic states $\phi_k^-(r;R)$ but with a different boundary condition in which $\mathcal{J}_k^I(r)$ stands for an outgoing wave function. The P operator expressed in these states has the same form as in Eq. (19). It should be noted here that, even if $\phi_d(r;R)$ is chosen to be independent of R, the background states $\phi_k^\pm(r;R)$ are always parametrically dependent on R because of the explicit R dependence of the operator $H_{\rm el}$.

Before proceeding further we denote the matrix elements of $V_0+H_{\rm el}$ in the basis $\{\phi_d, \phi_k^+\}$ as

$$V_d(R) = V_0(R) + \langle\phi_d|H_{\rm el}|\phi_d\rangle, \tag{20}$$

$$V_{dk}^+(R) = \langle\phi_d|H_{\rm el}|\phi_k^+\rangle, \tag{21}$$

$$\begin{aligned} V_{kk'}^+(R) &= \langle\phi_k^+|V_0(R) + H_{\rm el}|\phi_{k'}^+\rangle \\ &= (V_0(R) + k^2/2)\,\delta(k^2/2 - k'^2/2), \end{aligned} \tag{22}$$

where the last equality follows from Eq. (18) and energy normalization of the continuum states. It is important to realize that $V_{kk'}^+$ is diagonal only because of the appropriate choice of $\phi_k^+(r)$. It will be shown later that this choice is necessary to get the effective one-dimensional equation describing the nuclear dynamics in a nonlocal potential. In addition to the matrix element $V_{dk}^+(R)$, we will need a matrix element

$$V_{dk}^-(R) = \langle\phi_d|H_{\rm el}|\phi_k^-\rangle \tag{23}$$

to define the background and resonant T matrix for vibrational excitation.

B. Background and resonant T matrices for vibrational excitation

We begin by writing the full Hamiltonian given by Eq. (5) in the form

$$H = H_0 + V_1 + V_2, \tag{24}$$

where H_0 is given by Eq. (6), and

$$V_1 = PH_{\rm el}P - T_r - \frac{l(l+1)}{2r^2} = PH_{\rm el}P - H_{\rm el} + V_{\rm int}, \tag{25}$$

$$V_2 = H_{\rm el} - PH_{\rm el}P. \tag{26}$$

The motivation for the choice of V_1 is to express the T matrix (more precisely, only its *resonant* part) in terms of $|\chi_v\phi_k^+\rangle$ instead of the unperturbed initial or final state $|\chi_v\mathcal{J}_k^I\rangle$. We can easily see that the state $|\chi_{v_i}\phi_{k_i}^+\rangle$ is an eigenfunction of

$$H_0 + V_1 = T_R + V_0 + PH_{\rm el}P \tag{27}$$

within the Born-Oppenheimer approximation, which will be defined explicitly later [see Eq. (48) below].

By employing the two-potential formula for the scattering T matrix (see [16], p. 202) we get

$$T_{v_i\to v_f}^{\rm VE} = \langle\chi_{v_f}\phi_{k_f}^-|V_1|\chi_{v_i}\mathcal{J}_{k_i}^I\rangle + \langle\chi_{v_f}\phi_{k_f}^-|V_2|\Psi^+\rangle, \tag{28}$$

where $\Psi^+(R,r)$ is given by Eq. (8), or equivalently, apart from the Born-Oppenheimer approximation used for the perturbed initial state, by

$$|\Psi^+\rangle = |\chi_{v_i}\phi_{k_i}^+\rangle + \frac{1}{E - H + i\eta}V_2|\chi_{v_i}\phi_{k_i}^+\rangle. \tag{29}$$

The last equation shows that we can take $\chi_{v_i}(R)\phi_{k_i}^+(r;R)$ as the initial state of the system to determine the wave function

$\Psi^+(R,r)$, which we will use later to derive the effective equation for the nuclear dynamics.

The second term of Eq. (28) corresponds to the resonant part of the T matrix as defined in [6] and is fully determined by the resonant part $Q\Psi^+$ of the full wave function defined below in Eq. (40). Using Eqs. (16), (23), and (26), and the orthogonality $\langle\phi_k^-|\phi_d\rangle=0$, we obtain

$$T^{\rm res}_{v_{\rm i}\to v_{\rm f}}=\langle\chi_{v_{\rm f}}\phi^-_{k_{\rm f}}|H_{\rm el}-PH_{\rm el}P|\Psi^+\rangle=\langle\chi_{v_{\rm f}}\phi^-_{k_{\rm f}}|PH_{\rm el}Q|\Psi^+\rangle. \tag{30}$$

This expression can be further simplified if we define $\Psi^+_d(R)=\langle\phi_d|\Psi^+\rangle_r$ where $\langle\cdots\rangle_r$ means an integration over the electronic coordinate r only. In terms of the resonant nuclear wave function Ψ^+_d, for which we will derive the effective Schrödinger equation in the following subsection, the resonant part of the T matrix can be written as

$$T^{\rm res}_{v_{\rm i}\to v_{\rm f}}=\langle\chi_{v_{\rm f}}|V^{-*}_{dk_{\rm f}}|\Psi^+_d\rangle. \tag{31}$$

Note that this expression differs slightly from the result of Domcke [Ref. [6], Eq. (4.14)] where the matrix V_{dk} without a superscript, which corresponds to the matrix element V^+_{dk} defined by Eq. (21), was, in our opinion, used incorrectly. This small difference becomes important when the background terms defined below are added to the resonant T matrix, since the coupling matrix elements $V^{\pm}_{dk}$ are in general complex even when the discrete state is real. The reason why we cannot use V^+_{dk} instead of V^-_{dk} is that, in general, in spite of the fact that ϕ^-_k belongs to $\mathcal{P}$ space,

$$\langle\phi^-_{k_{\rm f}}|\phi^+_k\rangle\neq\delta(k_{\rm f}^2/2-k^2/2), \tag{32}$$

and therefore

$$\langle\phi^-_{k_{\rm f}}|PH_{\rm el}Q|\phi_d\rangle\neq\langle\phi^+_{k_{\rm f}}|H_{\rm el}|\phi_d\rangle. \tag{33}$$

Instead, if we consider a special case of the *real* discrete state and if we realize that for the radial case with a real discrete state

$$\phi^-_k(r)=(\phi^+_k(r))^*, \tag{34}$$

we can simplify the matrix element between electronic wave functions in (30) as

$$\langle\phi^-_{k_{\rm f}}|PH_{\rm el}Q|\phi_d\rangle=\langle\phi^-_{k_{\rm f}}|H_{\rm el}|\phi_d\rangle=\langle\phi_d|H_{\rm el}|\phi^+_{k_{\rm f}}\rangle=V^+_{dk_{\rm f}}, \tag{35}$$

where we assumed that $H_{\rm el}$ is a Hermitian operator. Note that in this special case we can use the matrix element V^+_{dk} but *without complex conjugation*. In the three-dimensional case, Eq. (34) must be modified to

$$\phi^-_{\vec{k}}=(\phi^+_{-\vec{k}})^*, \tag{36}$$

and thus $V^*_{d\vec{k}}$ in Eq. (4.14) of [6] should be replaced by $V_{d,-\vec{k}}$ under the assumption that ϕ_d is real, otherwise $V^{-*}_{d\vec{k}}$ must be used.

We now return to Eq. (28). Its first term is generally called the *background* scattering T matrix and reads

$$\begin{aligned}T^{\rm bg}_{v_{\rm i}\to v_{\rm f}}&=\langle\chi_{v_{\rm f}}\phi^-_{k_{\rm f}}|PH_{\rm el}P-H_{\rm el}+V_{\rm int}|\chi_{v_{\rm i}}\mathcal{J}^l_{k_{\rm i}}\rangle\\&=\langle\chi_{v_{\rm f}}\phi^-_{k_{\rm f}}|V_{\rm int}-PH_{\rm el}Q|\chi_{v_{\rm i}}\mathcal{J}^l_{k_{\rm i}}\rangle\\&=\langle\chi_{v_{\rm f}}\phi^-_{k_{\rm f}}|V_{\rm int}|\chi_{v_{\rm i}}\mathcal{J}^l_{k_{\rm i}}\rangle-\langle\chi_{v_{\rm f}}|V^{-*}_{dk_{\rm f}}\mathcal{J}^l_{dk_{\rm i}}|\chi_{v_{\rm i}}\rangle,\end{aligned} \tag{37}$$

where

$$\mathcal{J}^l_{dk_{\rm i}}(R)=\int dr\,\phi^*_d(r;R)\mathcal{J}^l_{k_{\rm i}}(r) \tag{38}$$

is the overlap of the unperturbed incoming wave with the discrete state. These background terms are nonzero even for inelastic vibrational excitation, but generally small when compared to the resonant part of the T matrix. For an example where these terms are not negligible, see the results for the F_2-like model in Sec. VI below.

C. Nuclear wave equation

To derive the equation that determines the effective nuclear dynamics in the nonlocal model, we begin by defining the outgoing, scattered wave part of the full wave function,

$$\Psi^+_{\rm sc}(R,r)=\Psi^+(R,r)-\chi_{v_{\rm i}}(R)\phi^+_{k_{\rm i}}(r). \tag{39}$$

Since $P+Q=1$ we can next write

$$\begin{aligned}\Psi^+_{\rm sc}(R,r)&=Q\Psi^+_{\rm sc}(R,r)+P\Psi^+_{\rm sc}(R,r)\\&=\Psi^+_d(R)\phi_d(r;R)+\int\Psi^+_k(R)\phi^+_k(r;R)k\,dk,\end{aligned} \tag{40}$$

where we have used Eqs. (15) and (19) and defined $\Psi^+_k(R)=\langle\phi^+_k|\Psi^+_{\rm sc}\rangle_r$, the $\mathcal{P}$ space counterpart of $\Psi^+_d(R)$. We next write Eq. (29) in differential form,

$$(E-H)|\Psi^+_{\rm sc}\rangle=(H_{\rm el}-PH_{\rm el}P)|\chi_{v_{\rm i}}\phi^+_{k_{\rm i}}\rangle. \tag{41}$$

By using Eq. (40) and projecting on the above equation, first with the discrete state $\langle\phi_d|$ and then with the background scattering states $\langle\phi^+_k|$, we obtain a set of coupled equations,

$$\begin{aligned}&E\Psi^+_d(R)-T_R\Psi^+_d(R)-V_d(R)\Psi^+_d(R)-\int V^+_{dk}(R)\Psi^+_k(R)k\,dk\\&=V^+_{dk_{\rm i}}(R)\chi_{v_{\rm i}}(R),\end{aligned} \tag{42}$$

$$\begin{aligned}&E\Psi^+_k(R)-T_R\Psi^+_k(R)-V^+_{dk}(R)^*\Psi^+_d(R)\\&\quad-\int V^+_{kk'}(R)\Psi^+_{k'}(R)k'dk'=0,\end{aligned} \tag{43}$$

where we used definitions (20)–(22) and the orthonormality of the electronic basis, and where we approximated the terms containing the nuclear kinetic energy operator T_R as

$$\int dr\,\phi^*_d(r;R)T_R\phi_d(r;R)\Psi^+_d(R)\simeq T_R\Psi^+_d(R), \tag{44}$$

$$\int dr\,\phi^*_d(r;R)T_R\phi^+_k(r;R)\Psi^+_k(R)\simeq 0, \tag{45}$$

$$\int dr(\phi_k^+(r;R))^* T_R \phi_d(r;R)\Psi_d^+(R) \simeq 0, \tag{46}$$

$$\int dr(\phi_k^+(r;R))^* T_R \phi_k^+(r;R)\Psi_k^+(R) \simeq T_R\Psi_k^+(R). \tag{47}$$

This approximation requires the discrete state $\phi_d(r;R)$ and the background continuum states $\phi_k^+(r;R)$ to depend smoothly on the internuclear distance R, so that their derivatives with respect to R,

$$\frac{\partial\phi_d(r;R)}{\partial R} \simeq 0, \quad \frac{\partial\phi_k^+(r;R)}{\partial R} \simeq 0, \tag{48}$$

are negligible when compared to the derivatives of the nuclear wave functions $\Psi_d^+(R)$ and $\Psi_k^+(R)$. In accord with O'Malley [17], we consider these conditions to be equivalent to the statement that we employ the Born-Oppenheimer approximation in all nonlocal approximation calculations. We should contrast this statement with the view expressed by Domcke *et al.* [6,18], who claim that the nonlocal resonance theory goes beyond the Born-Oppenheimer approximation by taking into account the nonlocality of the effective potential, and thus includes some non-Born-Oppenheimer effects.

The last term in Eq. (43) can be simplified because of the definition of $\phi_k^+(r;R)$ in Eq. (18). By using Eq. (22) we obtain

$$\int V_{kk'}^+(R)\Psi_{k'}^+(R)k'dk' = [V_0(R) + k^2/2]\Psi_k^+(R). \tag{49}$$

Note that, if we were to choose the electronic basis $\{\phi_d, \phi_k^+\}$ completely independent of R, making all nonadiabatic terms neglected in Eqs. (44)–(47) exactly zero, the continuum-continuum coupling $V_{kk'}^+$ would be inevitably nondiagonal and difficult to deal with.

Using (49) we can formally solve Eq. (43) and write

$$\Psi_k^+(R) = \int dR' G_0^+(E,R,R')V_{dk}^+(R')^*\Psi_d^+(R'), \tag{50}$$

where

$$G_0^+(E) = (E - T_R - V_0 - k^2/2 + i\eta)^{-1}. \tag{51}$$

By inserting this expression into (42) we finally get the familiar working equation of the nonlocal approximation,

$$[E - T_R - V_d(R)]\Psi_d^+(R) - \int dR' F(E,R,R')\Psi_d^+(R') = V_{dk_i}^+(R)\chi_{v_i}(R), \tag{52}$$

with the nonlocal, complex, and energy-dependent potential

$$F(E,R,R') = \int dR' \int V_{dk}^+(R)G_0^+(E,R,R')V_{dk}^+(R')^* k\, dk. \tag{53}$$

Once the solution Ψ_d^+ of Eq. (52) is obtained, it can be used to evaluate the *resonant* part of the T matrix with Eq. (31) and the corresponding resonant contribution to the vibrational excitation cross section via Eq. (13).

The dissociative attachment cross section is determined solely from the asymptotic behavior of Ψ_d^+, using the formula

$$\sigma_{v_i}^{\mathrm{DA}}(E) = \frac{2\pi^2}{k_i^2}\frac{K_{\mathrm{DA}}}{\mu}\lim_{R\to\infty}|\Psi_d^+(R)|^2, \tag{54}$$

which, apart from the Born-Oppenheimer approximations made in the process of deriving Eq. (52), is equivalent to Eq. (14). The proof of this assertion is given in the Appendix. Within the nonlocal approximation, there are no contributions to the dissociative attachment cross section similar to the background terms of the T matrix in Eq. (37) for vibrational excitation. This observation will be seen to have significant consequences.

IV. EXACT SOLUTION AND IMPLEMENTATION OF THE NONLOCAL APPROXIMATION USING EXTERIOR COMPLEX SCALING

As in I, we have made use of the exterior complex scaling (ECS) method with an implementation that combines finite elements with the discrete-variable representation (DVR), as developed by Rescigno and McCurdy [2,3]. We employed this method to numerically solve both the two-dimensional problem and the nonlocal nuclear wave equation [Eq. (52)]. In I we provided details of how this method was implemented for the two-dimensional problem and how the cross sections can be extracted from the wave functions via surface integrals. Here we focus on how the ECS method can be used to compute the nonlocal potential of Eq. (53) and to solve Eq. (52).

The problem of evaluating the nonlocal potential in Eq. (53) is usually resolved by expansion of the Green's function [Eq. (51)] into eigenstates of $T_R + V_0(R)$, which are the molecular vibrational states $\chi_v(R)$. But such an expansion leads to a singular integral over electron energies, which is difficult to treat unless one assumes a particular energy dependence of the discrete-state–continuum coupling $V_{dk}^+(R)$ to be able to evaluate this singular integral analytically (see, e.g., Ref. [6]).

In order to perform calculations in the nonlocal approximation for an arbitrary discrete state $\phi_d(r;R)$ and to avoid any assumptions about the energy dependence of the coupling $V_{dk}^+(R)$ when evaluating the nonlocal potential [Eq. (53)] we have made use of the ECS method together with a DVR basis for both the electronic and nuclear degrees of freedom to discretize the $\mathcal{P}$ space. The key step in the calculation is a scheme for evaluating the nonlocal operator $F(E,R,R')$ of Eq. (53), which we can write as

$$F(E,R,R') = \langle\phi_d|H_{\mathrm{el}}P\frac{1}{P(E - H_{\mathrm{el}} - T_R - V_0 + i\eta)P}PH_{\mathrm{el}}|\phi_d\rangle_r. \tag{55}$$

We discretize both the electronic ($[r_i]$) and nuclear ($[R_j]$) coordinates by introducing an exterior complex-scaled DVR basis for each degree of freedom. We then solve, for each

discrete value of the nuclear coordinate R_j, the electronic Born-Oppenheimer eigenvalue problem

$$\sum_k (PH_{\rm el}P)_{i,k}\phi_n(r_k;R_j) = E_n(R_j)\phi_n(r_i;R_j). \tag{56}$$

Note that the electronic operator P is here represented as a matrix in the electronic DVR basis (with associated quadrature weights w_i):

$$P(R_j)_{i,k} = \delta_{i,k} - Q(R_j)_{i,k}, \tag{57}$$

$$Q(R_j)_{i,k} = \sqrt{w_i}\phi_d(r_i;R_j)\phi_d(r_k;R_j)\sqrt{w_k}. \tag{58}$$

We thus obtain, for each value of the nuclear coordinate R_j, a set of discretized complex energies $E_n(R_j)$ lying in the fourth quadrant of the complex plane (see, for example, Ref. [19], Fig. 2). Because the complex-scaled operator $PH_{\rm el}P$ is symmetric, but not Hermitian, we have to use for the wave functions $\phi_n(r;R)$ the scalar product defined without complex conjugation. The coupling elements $V_{dn}(R_j)$ between the discrete state and the discretized continuum states can then be approximated as

$$\begin{aligned} V_{dn}(R_j) &= \int dr\ \phi_d(r;R_j)H_{\rm el}(r,R_j)\phi_n(r;R_j) \\ &= \int dr\ \phi_n(r;R_j)H_{\rm el}(r,R_j)\phi_d(r;R_j) \\ &\approx \sum_{i,k} \sqrt{w_i}\phi_d(r_i;R_j)H_{\rm el}(R_j)_{i,k}\phi_n(r_k;R_j)\sqrt{w_k}, \end{aligned} \tag{59}$$

where, to simplify the discussion, we have assumed that the discrete state is real and localized in the inner region where the electronic coordinate is not complex scaled.

Having calculated the complex electronic potential curves $E_n(R_j)$ and coupling terms $V_{dn}(R_j)$, we can complete the evaluation of the nuclear Green's function by constructing

$$F(E,R_i,R_j) = \sum_n \sqrt{W_i}V_{dn}(R_i)M(n)^{-1}_{i,j}V_{dn}(R_j)\sqrt{W_j}, \tag{60}$$

where the weights in Eq. (60) are those associated with the nuclear DVR basis, and $M(n)$ is the matrix representation of the operator for nuclear motion in this representation:

$$M(n)_{i,j} = [E - T_R - V_0(R) - E_n(R)]_{i,j}. \tag{61}$$

Note that we have avoided singularities in constructing the inverse of $M(n)$ since the energies $E_n(R)$ are complex whereas the total energy E of the system is always real.

Having constructed $F(E,R_i,R_j)$, we can then solve the nuclear wave equation [Eq. (52)] in the same nuclear DVR representation. Note that the coupling element $V^+_{dk}(R)$ appearing on the right-hand side of Eq. (52) and in the T matrices in Eqs. (31) and (37) are at specific *real* electron energies and hence must be evaluated directly using Eq. (21) where the background continuum function $\phi^+_k(r;R)$ is obtained by solving Eq. (18) in the electronic DVR basis under exterior complex scaling.

TABLE I. Parameters of the N_2-, NO-, and F_2-like models, given in atomic units, so that the resulting potential $V(R,r)$ is in hartrees.

Parameter	N_2	NO	F_2
μ	12 766.36	13 614.16	17 315.99
l	2 (d wave)	1 (p wave)	1 (p wave)
D_0	0.75102	0.2363	0.0598
α_0	1.15350	1.5710	1.5161
R_0	2.01943	2.1570	2.6906
λ_∞	6.21066	6.3670	18.8490
λ_1	1.05708	5.0000	3.2130
R_λ	−27.9833	2.0843	1.8320
λ_c	5.38022	6.0500	18.1450
R_c	2.40500	2.2850	2.5950
α_c	0.40000	1.0000	3.0000

V. SPECIFIC TWO-DIMENSIONAL MODELS

In the next section, we investigate the accuracy of the nonlocal approximation and compare it with exact results of the two-dimensional calculations. For that purpose we constructed two-dimensional models for electronic collisions with N_2, NO, and F_2 molecules. We used the same parametrization of the N_2-like and NO-like models as in I and constructed another model for the molecule F_2. Functions specifying the interaction between electronic and nuclear degrees of freedom in all models are of the form

$$V_0(R) = D_0(e^{-2\alpha_0(R-R_0)} - 2e^{-\alpha_0(R-R_0)}), \tag{62}$$

$$V_{\rm int}(r,R) = -\lambda(R)e^{-\alpha(R)r^2}, \tag{63}$$

$$\lambda(R) = \lambda_\infty + \frac{\lambda_0}{1+e^{\lambda_1(R-R_\lambda)}}, \tag{64}$$

$$\lambda_0 = (\lambda_c - \lambda_\infty)(1+e^{\lambda_1(R_c-R_\lambda)}), \tag{65}$$

$$\alpha(R) = \alpha_c, \tag{66}$$

and numerical values of the adjustable parameters are listed in Table I.

The resulting two-dimensional potentials $V(R,r)$ and corresponding potential energy curves for the N_2-like and NO-like models can be found in paper I, Figs. 2 and 3. The basic characteristics of the two-dimensional potential of the F_2-like model shown in Fig. 1 are similar to the N_2 and NO models, but in this case the potential well into which the electron is captured (in the region where $r \leqslant 2$) is much deeper at larger internuclear distances, corresponding to the large electron affinity of fluorine.

In Fig. 2 we plot the potential energy curves for the F_2-like model with several vibrational states. The curve labeled $V_0(R)$ is the potential energy of the neutral molecule

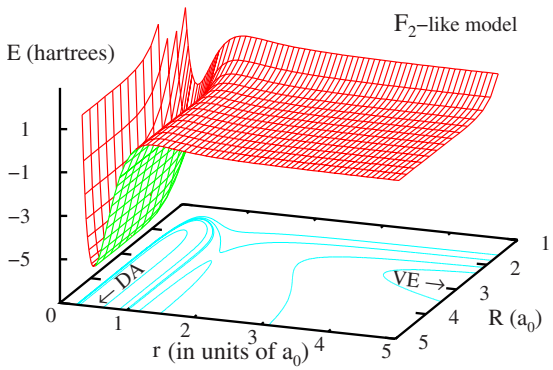

FIG. 1. (Color online) Effective two-dimensional potential $V_0(R)+l(l+1)/2r^2+V_{\rm int}(R,r)$ for the F_2-like model. Internuclear distances are given in units of the Bohr radius $a_0=5.291\,772\,1\times10^{-11}$ m. Energies are in units of hartrees, where 1 hartree $=4.359\,748\times10^{-18}$ J.

and is plotted along with the local, adiabatic potential curve of the anion, $E(R)\equiv E_{\rm res}(R)-i\Gamma(R)/2$, which is simply $V_0(R)$ plus the resonance eigenvalue of $H_{\rm el}$ under complex scaling. The potential of the molecular anion is complex for $R<R_c$, and the width $\Gamma(R)$ is illustrated by the shaded area around the real part $E_{\rm res}(R)$ of the potential. Note that the asymptote of the molecular-anion potential energy curve lies deeply below the ground vibrational state of the neutral molecule (as in the real electron-F_2 system) and therefore, as we will see below, there is no threshold in the dissociative attachment cross section and no oscillatory structure in the vibrational excitation cross sections (in contrast with the NO-like model).

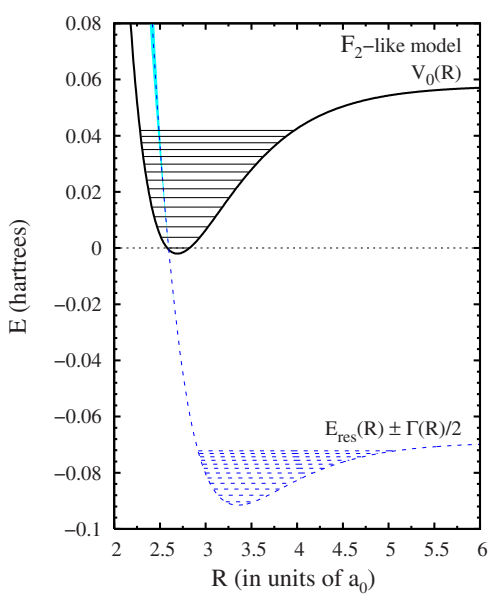

FIG. 2. (Color online) Target and anion potential energy curves for the F_2-like model with only some vibrational states plotted. Energies E are in units of hartrees and internuclear distances R are in units of a_0. Shaded area illustrates the width $\Gamma(R)$ associated with the complex anion potential (see text).

VI. SENSITIVITY OF THE NONLOCAL APPROXIMATION TO CHOICE OF THE DISCRETE STATE

It is not our purpose here to test the various methods that have been proposed to determine the discrete state (such as a stabilization method [8,9], applied to electron collisions with H_2 [18] and N_2 [20] molecules, or a recently proposed Feshbach-Fano R matrix method [10,11]), but rather to show the sensitivity of the cross sections computed with the nonlocal model with several well-defined choices for the discrete state.

In general, the discrete state for large internuclear distances should become the bound state of the electron attached to one of the atoms

$$\lim_{R\to\infty}\phi_d(r;R)=\phi_b(r), \tag{67}$$

where ϕ_b is defined by Eq. (11). Because the bound state is the eigenfunction of $H_{\rm el}$, the discrete-state–continuum coupling $V_{dk}(R)$ goes to zero [see Eq. (21)] as $R\to\infty$. If we were to choose the discrete state differently we would get a nonzero discrete-state–continuum coupling even for very large internuclear distances, which has no physical meaning. Therefore we define all discrete states to satisfy the condition (67).

We will consider three specific examples in the following sections. We first show that an *intuitive* choice of the discrete state is not generally optimal because it can change rapidly with internuclear distance in the resonant region. We then consider an R-independent discrete state, which produces essentially exact results, but only if the background T matrix terms [Eq. (37)] are included for elastic and vibrational excitation. Finally, we choose a discrete state that varies smoothly with the internuclear distance and observe that under certain circumstances the background terms can be very small and the resonant term obtained within the nonlocal approximation can be sufficient to reproduce the exact results for inelastic collisions.

A. "Intuitive" choice of discrete state: Breakdown of the Born-Oppenheimer approximation

Since the nonlocal approximation assumes the existence of a resonant electronic state which can be approximated by a square-integrable function, one might think that the best results would be obtained if the discrete state were to be chosen as a close approximation to the fixed-nuclei–electron scattering wave function calculated at the resonant energy.

The resonant energy can be determined at each internuclear distance R, as it was in I, using the exterior complex scaling method. When this energy is real and negative, it is the energy of the electronic bound state, which we can define as the discrete state. When the energy is complex, we choose its real part to solve the electron scattering problem and truncate *smoothly* the obtained wave function at an arbitrary distance r_d, with the restriction that r_d be sufficiently large to get a proper limit [Eq. (67)]. To obtain a discrete state that varies smoothly with the internuclear distance R at the crossing point, we multiply the discrete state defined via the scattering wave function by the appropriate factor $\exp[-i\delta(R)]$ to make it real and to normalize it to unity.

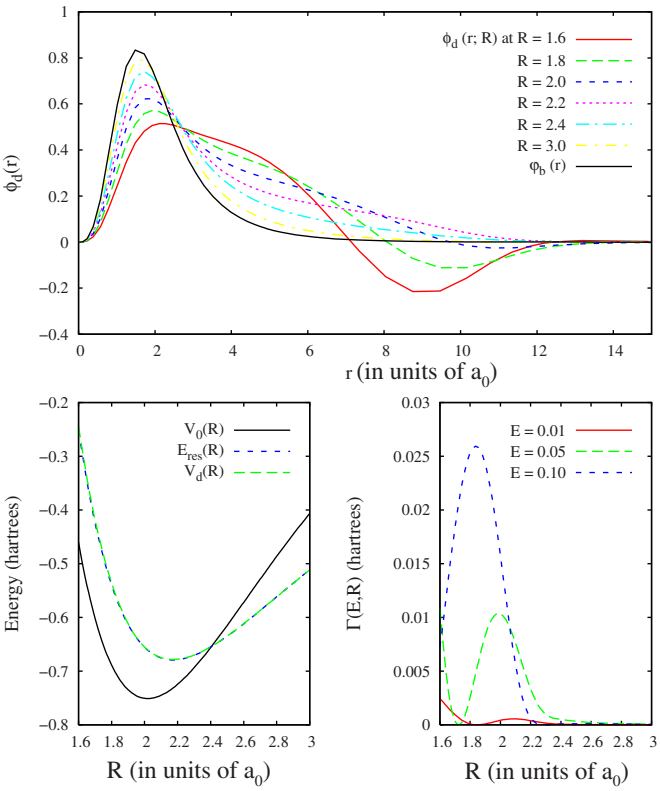

FIG. 3. (Color online) N_2-like model with the physical choice of the discrete state. Upper panel: the discrete state, in units of $a_0^{-1/2}$, at several internuclear distances; Lower left panel: the potential energy curve of the neutral molecule, $V_0(R)$ (solid line), the real part of the local complex potential of the molecular anion, $E_{res}(R)$ (short dashed line), and the discrete-state potential $V_d(R)$ (long-dashed line), which in this case almost coincides with $E_{res}(R)$; Lower right panel: the R dependence of the width defined by Eq. (68) at energies 0.01, 0.05, and 0.10 hartrees.

In Fig. 3, we plot the resulting discrete state for the N_2-like model for several internuclear distances (upper panel) together with the corresponding discrete-state potential $V_d(R)$ (lower left panel) and energy-dependent resonance width defined as

$$\Gamma(E,R) = 2\pi|V_{dk}^{+}(R)|^2, \quad E = k^2/2. \tag{68}$$

The cutoff function was chosen as

$$f(r) = 1 - \frac{1}{1 + e^{-(r-r_d)}} \tag{69}$$

where $r_d = 10a_0$. Although the discrete-state potential $V_d(R)$ is smooth and almost coincides with the real part of the local complex potential defined in I, the discrete state $\phi_d(r;R)$ and the discrete-state–continuum coupling $V_{dk}^{+}(R)$ evidently change rapidly for small internuclear distances, suggesting that the Born-Oppenheimer approximation introduced in Eqs. (44)–(48) could break down.

The vibrational excitation cross sections from the ground state to final states $v_f = 0,1,8$ for the N_2-like model are plotted in Fig. 4. In this and the following figures we compare

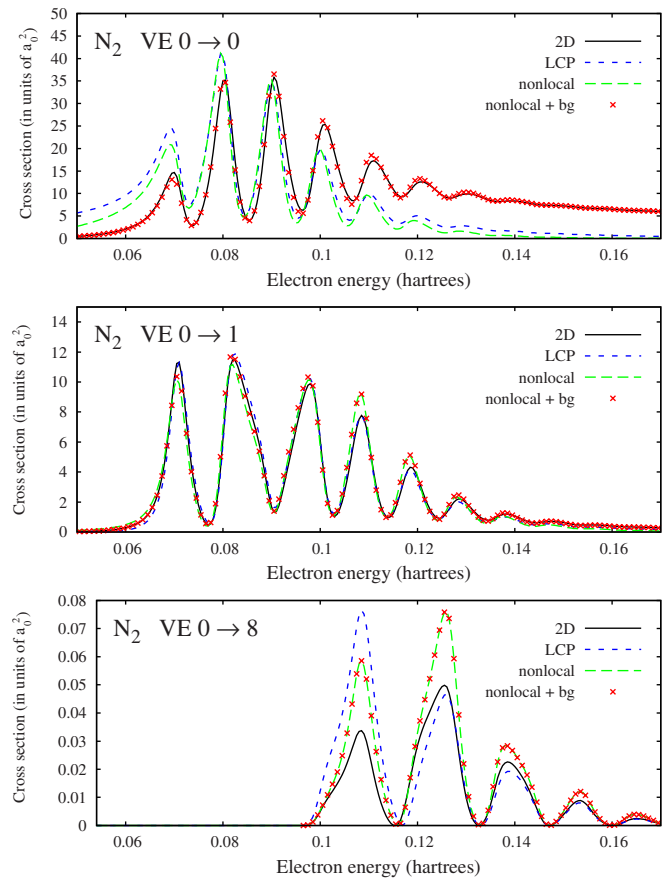

FIG. 4. (Color online) Vibrationally elastic (top panel) and inelastic ($0 \to 1$, middle panel, and $0 \to 8$, bottom panel) cross sections, in units of a_0^2, for the N_2-like model. The exact cross sections for our two-dimensional model (solid line) are compared with cross sections obtained using the local complex potential approximation (short-dashed line) and the nonlocal approximation without (long-dashed line) and with (crosses) the background terms. The discrete state was chosen as the resonant scattering wave function cutoff around $r = 10a_0$ (see text for details).

the results of calculations obtained using the exact two-dimensional model (full curve), the local complex potential approximation investigated in I (short-dashed curve), and the nonlocal approximation with (crosses) and without (long-dashed curve) the background terms in Eq. (37). As one might expect for this benchmark case, the agreement between the exact and approximate results is rather good, but not perfect. Not surprisingly, the importance of background scattering to the cross sections is seen to decrease with increasing inelasticity, but there is still a nonzero contribution for $0 \to 1$ vibrational excitation. As the vibrational excitation cross section to higher vibrational states becomes smaller, the discrepancies increase due to the breakdown of the Born-Oppenheimer approximation (48).

Similar results were obtained for the NO- and F_2-like models, as seen in Figs. 5 and 6. In these cases the variation of the discrete state with R is greater than in the N_2-like model due to the rapid increase of the resonant energy with decreasing internuclear distance. Differences between the ex-

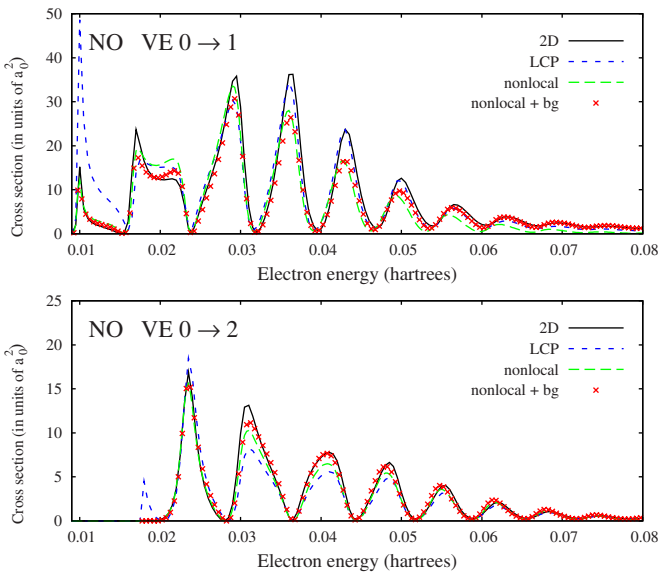

FIG. 5. (Color online) As in Fig. 4, with vibrational excitation cross sections for the NO-like model.

act and model cross sections are correspondingly more pronounced. Large differences are also seen in the dissociative attachment cross sections, shown in the lower panel of Fig. 6. This is a clear demonstration of the breakdown of the Born-Oppenheimer approximation, since, as we have shown, there is no background contribution to this process in the nonlocal approximation. Note that the threshold behavior of the cross sections is correct in the nonlocal approximation due to the energy dependence of the coupling V_{dk}^{+} and nonlocal potential of Eq. (53), unlike in the local complex potential approximation where the resonance width is energy independent (see I).

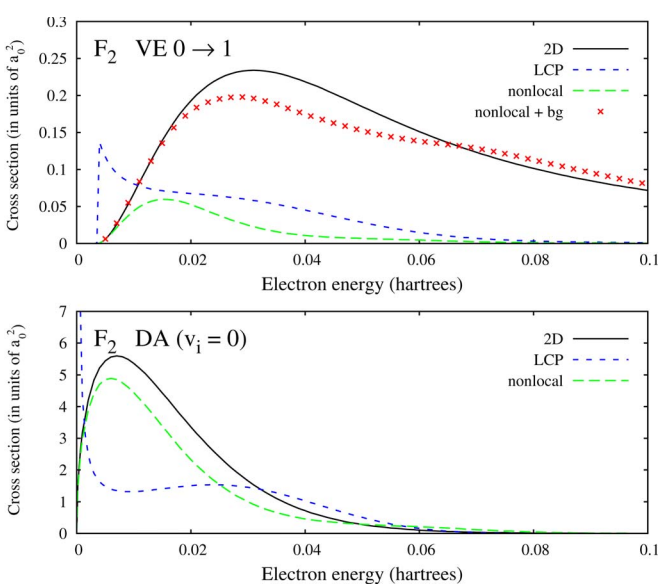

FIG. 6. (Color online) As in Fig. 4, with $0 \rightarrow 1$ vibrational excitation (top panel) and dissociative electron detachment (bottom panel) cross sections for the F_2-like model.

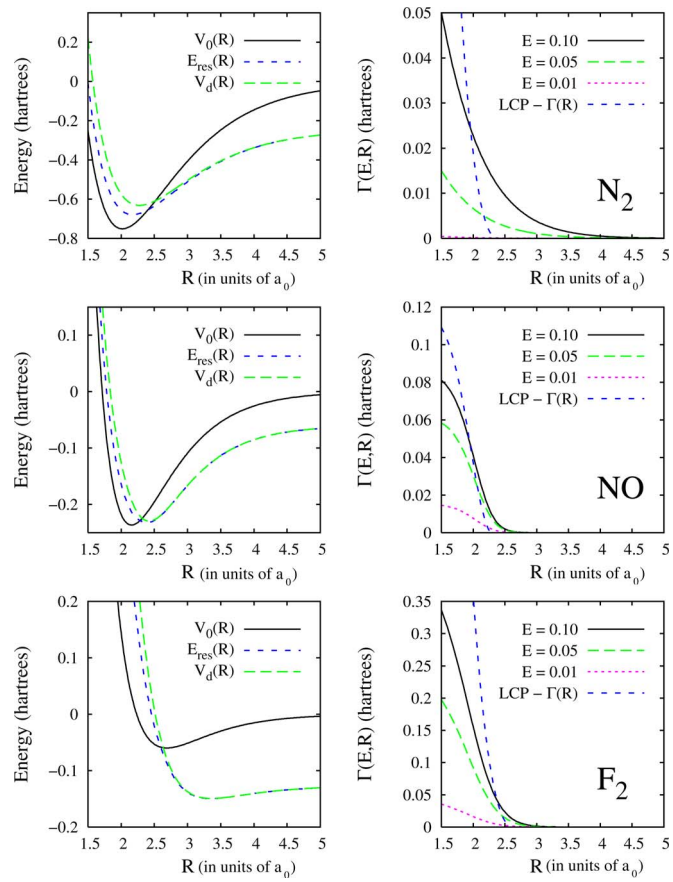

FIG. 7. (Color online) Potential energy curve of the neutral molecule, $V_0(R)$ (solid line), the real part of the local complex potential of the molecular anion, $E_{\mathrm{res}}(R)$ (short-dashed line), and the discrete-state potential $V_d(R)$ (long-dashed line), for the N_2-, NO-, and F_2-like models (left panels). The R dependence of the width defined by (68) at energies 0.01, 0.05, and 0.10 hartrees and the width $\Gamma(R)$ used in the local complex potential approximation calculations (right panels).

B. Discrete state independent of internuclear distance: Minimizing nonadiabatic terms and importance of background terms

The Born-Oppenheimer approximation can be validated and the effects of the nonadiabatic terms neglected in Eqs. (44)–(47) minimized by choosing the discrete state $\phi_d(r;R)$ to be independent of R. In that case, the approximations (44) and (46) are exact and the other two are expected to be valid as well because the electronic Hamiltonian H_{el} given by Eq. (17) is smoothly dependent on R, and the continuum states $\phi_k(r;R)$ are eigenstates of the operator $PH_{\mathrm{el}}P$, where P is now independent of R.

An obvious choice of the R-independent discrete state is the bound state $\phi_b(r)$ of the electron as $R \rightarrow \infty$, otherwise the condition of Eq. (67) would not be satisfied. In Fig. 7 we plot the discrete-state potential $V_d(R)$ for this particular choice together with the potential energy curves for all three models described in Sec. V (left panels) and the corresponding resonance widths as defined in Eq. (68) for three energies (right panels). We can see that, unlike in the previous section, the

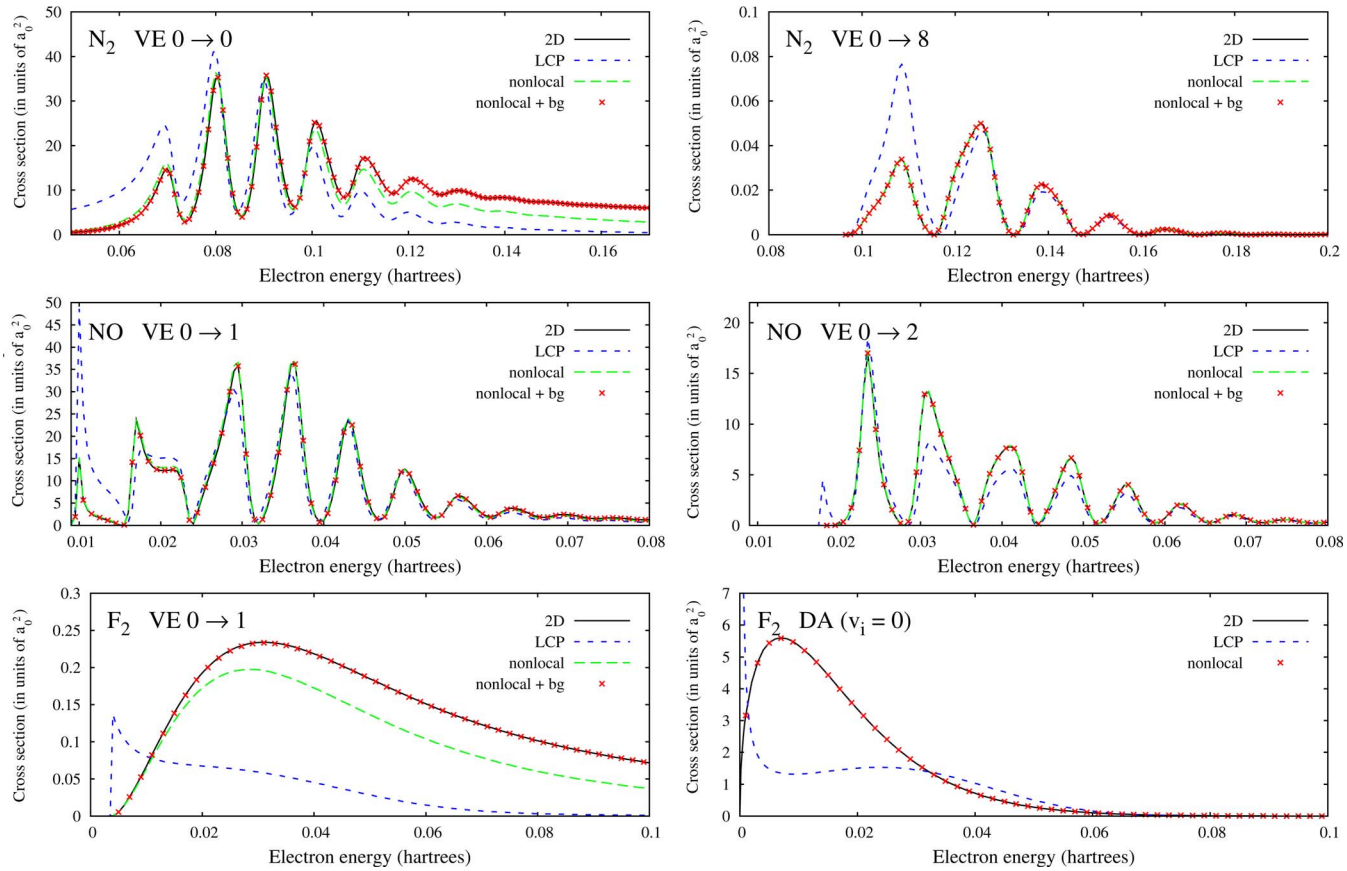

FIG. 8. (Color online) Comparison of the cross sections as in Figs. 4–6 for the discrete state chosen to be the bound state of the electron as $R \to \infty$ for all internuclear distances, i.e., independent of R. The vibrational excitation $0 \to 1$ cross section for the N_2-like model is omitted, because results of all calculations are practically the same in this particular case.

widths are smooth functions of the internuclear distance in all cases.

In Fig. 8 we show the cross sections for the same processes as in Figs. 4–6 (except for the $0 \to 1$ vibrational excitation in N_2 where the curves are graphically indistinguishable) obtained with the R-independent discrete state. The most striking feature we can observe in this figure is that in all cases the nonlocal approximation gives essentially exact cross sections if the background terms given by Eq. (37) are included. However, there are now cases where it does not suffice to consider only the resonant contribution [Eq. (31)] to the T matrix, not only for elastic scattering, but also for inelastic vibrational excitation (compare especially the cross sections for $0 \to 1$ vibrational excitation in the F_2-like model). For dissociative attachment, where there are no background contributions, the nonlocal model with an R-independent choice of discrete state gives exact results.

These results can be explained if we notice the increase in the resonance width from one system to another. The largest width is found in the F_2-like model and, because the background contribution to the cross section depends on this width through the coupling $V_{dk}^{-}(R)$ in Eq. (37), one might expect that the bigger the width, the more important the background contributions.

C. "Compact" discrete state varying smoothly with internuclear distance: Decreasing background terms

In view of the previous results, it is obvious to question whether it is possible to pick a discrete state which depends smoothly on R and for which the nonadiabatic effects and the background contributions to inelastic collisions are simultaneously small.

To address this question we compare the results obtained with the nonlocal model for several well-defined discrete states. To do that in a systematic way, we define $\phi_d(r;R)$ as the lowest-lying bound state of a certain electronic Hamiltonian which depends parametrically on R as in Eq. (17), only the function $\lambda(R)$ in Eq. (63) is changed in such a way that the resulting potential supports one bound state for all internuclear distances. Thus $\phi_d(r;R)$ satisfies

$$\left(T_r + \frac{l(l+1)}{2r^2} - \lambda_d(R)e^{-\alpha_c r^2}\right)\phi_d(r;R) = E_d\phi_d(r;R). \tag{70}$$

In our calculations we used two different functions $\lambda_d(R)$ to define $\phi_d(r;R)$. The first one is a slight modification of $\lambda(R)$ defining the two-dimensional model [see Eq. (64)],

$$\lambda_d(R) = \lambda_q(R) = \lambda_\infty + \frac{q\lambda_0}{1 + e^{\lambda_1(R-R_\lambda)}}, \tag{71}$$

which depends on a parameter q. Note that for $q=0$ we would obtain the same R-independent discrete state as in the previous section since $\lambda_d(R)=\lambda_\infty$. For sufficiently large $q>0$, we would get resonant states instead of bound states for small internuclear distances, and the definition of the discrete state would not be unambiguous. Therefore we take $q\leqslant 0$ which will be sufficient for our discussion. The second choice of $\lambda_d(R)$ given by

$$\lambda_d(R) = \lambda_{\text{spec}}(R) = \lambda_\infty + \frac{\lambda_{-\infty} - \lambda_\infty}{1 + e^{c_d(R-R_d)}} \tag{72}$$

is much more flexible, depending on three parameters $\lambda_{-\infty}$, c_d, and R_d (λ_∞ is given in Table I). Because the background contributions to the cross sections are largest for the F_2-like model, we will show results only for this specific model.

In Fig. 9, top panel, we plot $\lambda_q(R)$ for four different values of q ($q=0$, -0.5, -1.0, and -1.5), and $\lambda_{\text{spec}}(R)$ for two different values of $\lambda_{-\infty}$ [$\lambda_{-\infty}=23$ (denoted $\lambda_{\text{spec},1}$) and $\lambda_{-\infty}=25$ ($\lambda_{\text{spec},2}$)], with $c_d=1.5$ and $R_d=4$. These functions were used to define different discrete states for the F_2-like model, shown in the bottom panel for the internuclear distance $R=2.5a_0$. Corresponding discrete-state potentials $V_d(R)$ and resonance widths $\Gamma(E,R)$ for $E=0.1$ hartree are shown in the middle panels of this figure. Resonant contributions to the cross sections [see Eq. (31)] obtained using the nonlocal approximation defined by these discrete states are compared with the exact cross sections in Fig. 10. Note that we have included no background contributions in the data plotted in Fig. 10.

We observe that the resonant contribution to the cross sections can be very sensitive to the choice of the discrete state $\phi_d(r;R)$. Our first choice of $\lambda_d(R)=\lambda_q(R)$, which would seem to be quite reasonable [the discrete-state potential $V_d(R)$ follows closely the real part $E_{\text{res}}(R)$ of the local complex potential], gives rather satisfactory results (especially for q about -0.5), but much better agreement of the resonant contribution of the nonlocal approximation with the exact cross sections was obtained for counterintuitive choices of discrete states defined by $\lambda_{\text{spec}}(R)$ for which the discrete-state potential $V_d(R)$ is farther from $E_{\text{res}}(R)$. Notice in Fig. 9 that for $\phi_d(r;R)$ defined by $\lambda_{\text{spec}}(R)$ the resonance width $\Gamma(E,R)$ is a much smoother function of R than for the other choices of $\phi_d(r;R)$, especially in the region around the crossing point, which might be one reason why the background contributions given by Eq. (37) are much smaller in these particular cases.

We have thus found that the less intuitive choices for the discrete state, which result in relatively larger differences between $V_d(R)$ and $E_{\text{res}}(R)$ at small R, and which therefore shift more information about the system into the nonlocal part of the potential $F(E,R,R')$ rather than into $V_d(R)$, can give better results than the more intuitive choices. These nonintuitive choices apparently increase the resonant contribution relative to the background. In our particular model study, this happens when the discrete state is rather *compact* (more localized; see Fig. 9, bottom panel) compared with the bound state of the electron as $R\to\infty$ and with the resonant states used in Sec. VI A.

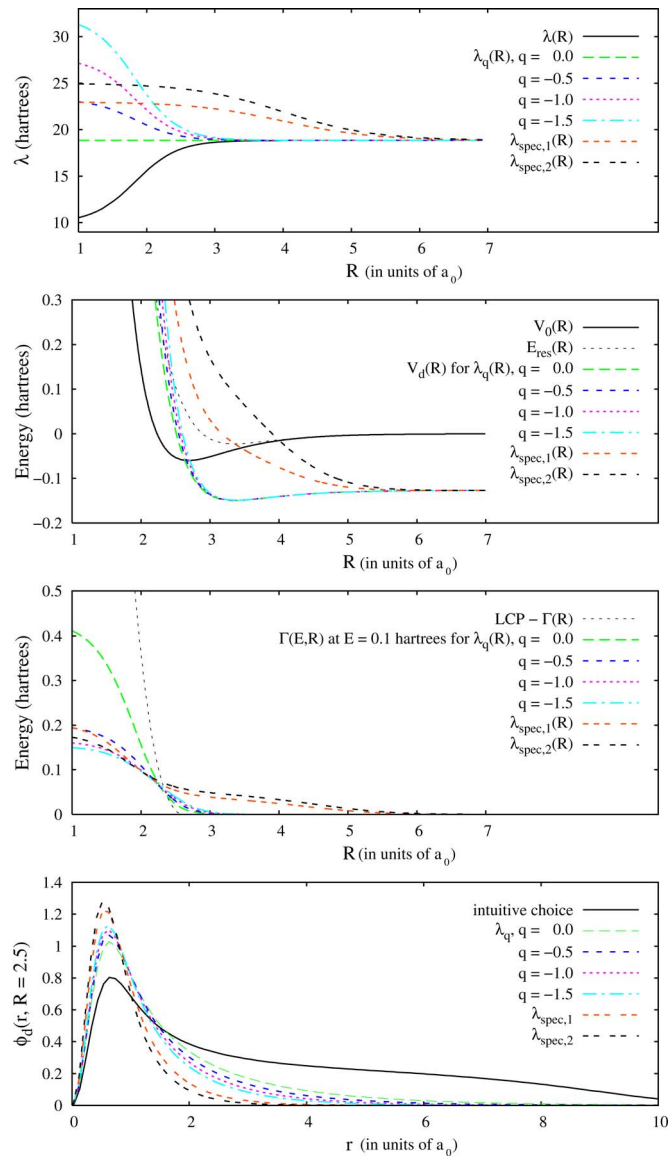

FIG. 9. (Color online) Top panel: $\lambda(R)$, which defines the interaction potential $V_{\text{int}}(r,R)$, and $\lambda_d(R)$, which defines the discrete state $\phi_d(r;R)$, for the F_2-like model. Middle panels: discrete-state potentials and R dependence of the resonance width $\Gamma(E,R)$ for $E=0.1$ hartree, corresponding to different discrete states defined by $\lambda_d(R)$. Bottom panel: discrete states at $R=2.5a_0$.

We should note that if we were to include the background contributions to the cross sections we would again get very good agreement with the exact cross sections in all cases except the one defined by $\lambda_q(R)$ with $q=-1.5$, where small discrepancies due to the breakdown of the Born-Oppenheimer approximation were found (we can see this in the dissociative attachment cross section in the bottom panel of Fig. 10).

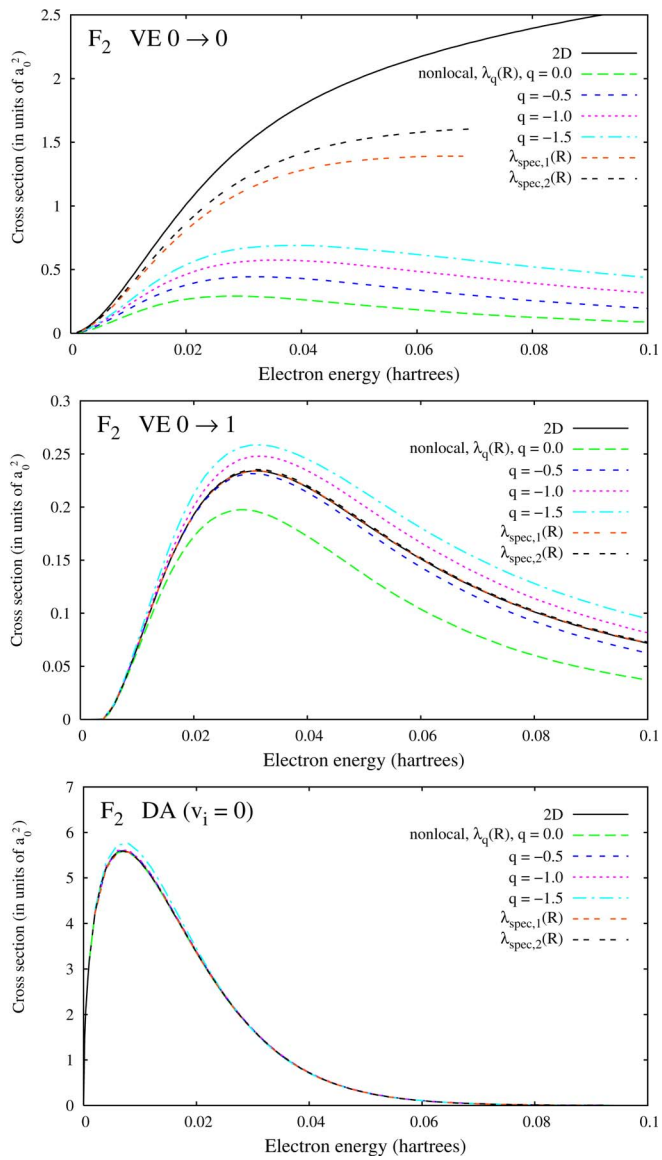

FIG. 10. (Color online) Elastic (top panel), vibrational excitation $0 \rightarrow 1$ (middle panel), and dissociative attachment (bottom panel) cross sections for the F_2-like model. The exact cross sections of the two-dimensional model (solid line) are compared with the resonant contribution [see Eq. (31)] to cross sections obtained using the nonlocal approximation with different choices of the discrete state (line types as in Fig. 9). Note that no background contributions are included in these results.

VII. CONCLUSION

In this work we have investigated, using the two-dimensional model introduced in I, the nonlocal approximation to the dynamics of resonant electron scattering from diatomic molecules. We have completely rederived the basic equations of the nonlocal approximation in the context of this two-dimensional model and have given explicit expressions for the background contributions to the vibrational excitation cross sections.

We have constructed three two-dimensional models similar to the real diatomic systems and used several well-defined discrete states to probe the relevance of the nonlocal approximation for the description of the studied processes. We have found that an inappropriate choice of the discrete state, though it would seem to be supported by physical assumptions of the theory of resonant processes, can lead to inaccurate results due to the breakdown of the Born-Oppenheimer approximation. On the other hand, if we pick a discrete state that is independent of, or varies smoothly with, the internuclear distance, then we can obtain cross sections within the nonlocal approximation that agree very well with the exact cross sections, not only for the case of dissociative attachment, but also for vibrational excitation. In the latter case, however, good agreement is guaranteed only if the background contributions to the vibrational excitation T matrix are taken into account.

Although we have been able to find for our two-dimensional model particular discrete states for which the background contributions are negligible, it is not clear that this will also be the case when we deal with a real diatomic system. Therefore, we suggest that new *ab initio* methods proposed to calculate the discrete-state potential $V_d(R)$ and the discrete-state–continuum coupling $V_{dk}^{+}(R)$ (such as, e.g., the Feshbach-Fano R matrix procedure [10,11]) should also consider developing tools for calculation of these background contributions to the vibrational excitation T matrix.

Because of the difficulty of incorporating the background contributions into the nonlocal resonance model [6], which does not define a discrete state explicitly but rather assumes some functional dependence for the discrete-state potential $V_d(R)$ and for the discrete-state–continuum coupling $V_{dk}^{+}(R)$, the parameters of which are usually found by fitting eigenphase sums for fixed-nuclei electron scattering, we did not use this approach here. Nevertheless, it would probably be worthwhile to see whether the nonlocal approximation defined by such a method would also give negligible background contributions for all inelastic processes, as is usually assumed.

Another important question which requires further study is when the nonlocal approximation breaks down. The only approximation we made in the process of derivation of the nonlocal approximation was the Born-Oppenheimer approximation expressed by Eq. (48). It was first used for the perturbed initial and final states, Eqs. (28) and (29), and later for matrix elements of the nuclear kinetic energy operator, Eqs. (44)–(47). Although one can always choose the discrete state to be slowly varying with or completely independent of the internuclear distance, it is not obvious that the background scattering states will also vary slowly, especially for polar molecules such as hydrogen halides for which the dipole interaction of the electron with the molecule can change rapidly with the internuclear distance. Moreover, the reduced mass of the molecule in all our models was quite large (greater than $10^4 m_e$); with hydrogen-containing diatomics, non-Born-Oppenheimer corrections are likely to be more important. Therefore, further tests of the nonlocal approximation using H_2-, HF-, or HCl_2-like two-dimensional models should be carried out.

In summary, we have found that the nonlocal model gives an excellent description of the scattering process in cases where the collision is well described by electron capture into

a compact, localized state. If this state varies smoothly with internuclear distance, then the conditions underlying the Born-Oppenheimer approximation are satisfied and the nonlocal model can work quite well in describing dissociative attachment, even close to threshold. For vibrational excitation, background contributions to the T matrix can become important in cases where the resonance width becomes large over nuclear geometries that lie within the Franck-Condon region of the initial state. The F_2 example presents such a situation for vibrational excitation. In such cases there can be considerable sensitivity of the computed cross sections to the choice of the discrete state, reflected in either large background contributions or a breakdown of the Born-Oppenheimer approximation. This may simply be a reflection of the fact that electron scattering in cases involving broad resonances is difficult to describe with a pure resonance model.

ACKNOWLEDGMENTS

This work was performed under the auspices of the U.S. Department of Energy under Contract No. DE-AC02-05CH11231 and was supported by the U.S. DOE Office of Basic Energy Sciences, Division of Chemical Sciences. Support from the Czech Science Foundation by Grant No. 202/07/0833 is gratefully acknowledged. C.W.M. was partially supported by the National Science Foundation (Grant No. PHY-0604628).

APPENDIX

Here we show explicitly that there are no background terms in the dissociative attachment cross section (except terms neglected due to the Born-Oppenheimer approximation) if the discrete state $\phi_d(r;R)$ [see Eq. (15)] is chosen properly to coincide with the electronic bound state $\phi_b(r)$ as $R\to\infty$ [see Eq. (11)].

To derive the formula (54) for the dissociative attachment cross section within the nonlocal approximation we begin with the exact cross section [see I, Sec. III B, for details, noting that the coefficient $4\pi/k_i$ was changed to $2\pi^2/k_i^2$ due to the energy normalization of the electronic continuum states, Eq. (3)] given by

$$\sigma_{v_i}^{DA}(E) = \frac{2\pi^2}{k_i^2}\lim_{R\to\infty}\int_0^\infty \vec{F}_{DA}(R,r)\cdot\vec{n}_R dr, \tag{A1}$$

where k_i is the momentum of an incoming electron and the flux $\vec{F}_{DA}$ projected into the dissociative attachment channel in the direction of a unit vector $\vec{n}_R$ for the molecular coordinate R can be written as

$$\vec{F}_{DA}\cdot\vec{n}_R = \frac{1}{2\mu i}\left((P_{DA}\Psi_{sc}^+)^*\frac{\partial}{\partial R}P_{DA}\Psi_{sc}^+ - P_{DA}\Psi_{sc}^+\frac{\partial}{\partial R}(P_{DA}\Psi_{sc}^+)^*\right). \tag{A2}$$

The expression (A1) for the cross section is equivalent to (14) where the T matrix is given by (10).

The projector operator P_{DA} is defined as

$$P_{DA}\Psi_{sc}^+(R,r) = \phi_b(r)\int_0^\infty \phi_b^*(r')\Psi_{sc}^+(R,r')dr'. \tag{A3}$$

If we substitute Ψ_{sc}^+ from Eq. (40) and realize that only the limit as $R\to\infty$ is important for evaluation of the cross section, we obtain

$$\lim_{R\to\infty} P_{DA}\Psi_{sc}^+(R,r) = \phi_b(r)\lim_{R\to\infty}\Psi_d^+(R), \tag{A4}$$

under the assumption

$$\lim_{R\to\infty}\phi_d(r;R) = \phi_b(r). \tag{A5}$$

For the projected flux (A2) we finally get

$$\lim_{R\to\infty}\vec{F}_{DA}\cdot\vec{n}_R = \frac{K_{DA}}{\mu}|\phi_b(r)|^2\lim_{R\to\infty}|\Psi_d^+(R)|^2, \tag{A6}$$

where we have used

$$\lim_{R\to\infty}\frac{\partial}{\partial R}\Psi_d^+(R) = \lim_{R\to\infty} iK_{DA}\Psi_d^+(R), \tag{A7}$$

which follows from the asymptotic behavior of the scattered wave function [see I, Eq. (16)].

Because the electronic bound state $\phi_b(r)$ is normalized the integration over the electronic coordinate r in Eq. (A1) is trivial, and we finally obtain Eq. (54) for the dissociative attachment cross section.

[1] K. Houfek, T. N. Rescigno, and C. W. McCurdy, Phys. Rev. A **73**, 032721 (2006).
[2] T. N. Rescigno and C. W. McCurdy, Phys. Rev. A **62**, 032706 (2000).
[3] C. W. McCurdy, M. Baertschy, and T. N. Rescigno, J. Phys. B **37**, R137 (2004).
[4] D. T. Birtwistle and A. Herzenberg, J. Phys. B **4**, 53 (1971).
[5] L. Dubé and A. Herzenberg, Phys. Rev. A **20**, 194 (1979).
[6] W. Domcke, Phys. Rep. **208**, 97 (1991).
[7] T. F. O'Malley, Phys. Rev. **185**, 101 (1969).
[8] E. Holøien and J. Midtdal, J. Chem. Phys. **45**, 2209 (1966).
[9] A. U. Hazi and H. S. Taylor, Phys. Rev. A **1**, 1109 (1970).
[10] B. M. Nestmann, J. Phys. B **31**, 3929 (1998).
[11] P. Kolorenč, V. Brems, and J. Horáček, Phys. Rev. A **72**, 012708 (2005).
[12] B. A. Lippmann and T. F. O'Malley, Phys. Rev. A **2**, 2115 (1970).
[13] *Handbook of Mathematical Functions with Formulas, Graphs, and Mathematical Tables*, edited by M. Abramowitz and I. A. Stegun (Dover Publications, New York, 1972).

[14] H. Feshbach, Ann. Phys. (N.Y.) **5**, 357 (1958).
[15] H. Feshbach, Ann. Phys. (N.Y.) **19**, 287 (1962).
[16] M. L. Goldberger and K. M. Watson, *Collision Theory* (Wiley, New York, 1964).
[17] T. F. O'Malley, Adv. At. Mol. Phys. **7**, 223 (1971).
[18] M. Berman, C. Mündel, and W. Domcke, Phys. Rev. A **31**, 641 (1985).
[19] C. W. McCurdy and F. Martín, J. Phys. B **37**, 917 (2004).
[20] M. Berman and W. Domcke, Phys. Rev. A **29**, 2485 (1984).